D. Nafpaktitis
G. Hloupis
I. Stavrakas
F. Paterakis

J. Electrical Systems 7-4 (2011): 438-447

Regular paper

An Alternative Approach for PWM Modeling in Power Electronics Systems

In this paper, the basic mathematical properties of an alternative Pulse Width Modulation (PWM) strategy are revealed. Specifically, it is shown that average voltage produced from the approximation of a sinusoidal signal's intervals by rectilinear segments can be successfully substituted by the average voltage of corresponding pulses. From this understanding, a method is proposed to apply PWM for the production of required sinusoidal signal. Both theoretical and simulated results confirming this understanding are presented..

Keywords: PWM, firing times, mathematical modelling.

1. INTRODUCTION

Optimal design of pulse width modulated waveforms for single-phase inverters [1, 2] is a well-known challenge in industry. PWM signals are used in power electronics, control of electric machines and solid-state electric energy conversion [2, 3]. PWM is the most frequently used method in switching converters [4, 5]. There are many techniques available to modulate the pulse width of the control signal: voltage control duty cycle technique [6, 7], comparison of reference signal to constant frequency carrier [8, 9], space-vector and feedback techniques [10, 11], digitally controlled [12, 13] as well as current mode PWM circuits [14-16]. All approaches offers benefits and advantages in specific problems. Their common characteristic is that in the majority of cases complex circuits or algorithms used for implementation.

Towards to the direction of simplifying the implementation of a PWM based system, we present a new approach to PWM modelling. The current study describes a contribution to the theory and first results of optimal designed PWM waveforms based on well-defined equations. The new PWM strategy differs from the ordinary solutions due to its simplicity and because it eliminates the basic stage of comparison between sinusoidal and triangular signal.

2. FORMULATION

2.1 Approximating Sinusoidal Waveform Using Rectilinear Segments

The main idea behind the proposed PWM (NPWM hereafter) strategy is to substitute the average voltage produced from the approximation of a sinusoidal signal's intervals by rectilinear segments with the average voltage of a corresponding pulse. For this, initially, the calculation of both averages (from rectilinear approximations and from pulses) is dictated.

A sinusoidal signal can be approximated by using rectilinear segments as depicted in Fig.1. Following the notations presented there, the average voltage can be calculated as follows:

Corresponding author : hloupis@teiath.gr
Department of Electronics, Technological Educational Institute of Athens, Egaleo, 12210, Athens, Greece.

Copyright © JES 2011 on-line : journals/esrgroups.org/jes

For n=1,

$$U_1 = \frac{1}{2}\left[u(0)+u(d)\right] = \frac{1}{2}U_{\max}\left(\sin\omega\cdot 0+\sin\omega\cdot d\right) \tag{1}$$

For n=2,

$$U_2 = \frac{1}{2}U_{\max}\left(\sin\omega\cdot d+\sin\omega\cdot 2d\right) \tag{2}$$

For J intervals ($1 \le J \le n$),

$$U_J = \frac{1}{2}U_{\max}\left(\sin((J-1)\cdot\omega\cdot d)+\sin(J\cdot\omega\cdot 2d)\right) \tag{3}$$

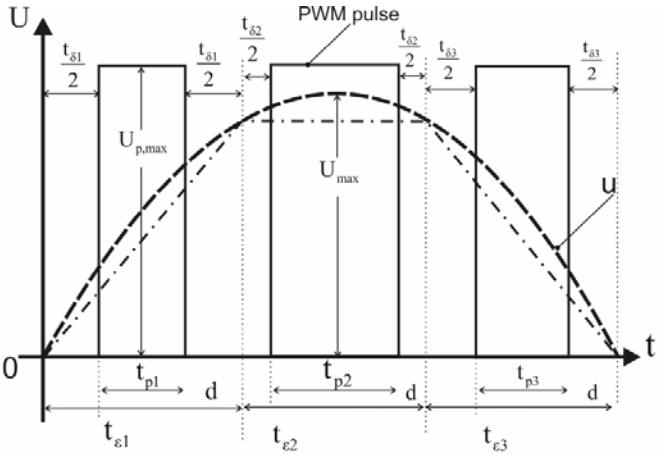

Figure 1. Approximation of sinusoidal voltage signal (dashed curve) by rectilinear segments (dot-dashed curve)

The average voltage from pulses can be calculated as follows:

For n=1

$$U_1 \cdot d = U_{p,\max}\cdot t_{p1} \Rightarrow U_1 = U_{p,\max}\cdot t_{p1}\big/ d \tag{4}$$

For J^{th} interval, it holds:

$$U_J = \frac{t_{pJ}}{d}U_{p,\max} \tag{5}$$

2.2 Implementation of the NPWM Strategy

In order to successfully approximate sinusoidal signal using PWM, two crucial parameters are needed to be formulated: the duration of each pulse and its firing time.

Using (3) and (5), the pulse duration t_{pJ} can be calculated as follows:

$$t_{pJ} = \frac{d}{2}\cdot\frac{U_{\max}}{U_{p\max}}\left\{\sin\left[\left(J-1\right)\omega\cdot d\right]+\sin(J\cdot\omega\cdot d)\right\} \tag{6}$$

The firing time $t_{\varepsilon J}$ (at J interval) can be calculated as follows:

For J=1, it holds:

$$t_{\varepsilon 1} = \frac{1}{2} t_{\delta 1} = \frac{1}{2}\left(d - t_{p1}\right) \Rightarrow t_{\varepsilon 1} = \frac{1}{2}\left(d - t_{p1}\right) \tag{7}$$

For J=2, it holds:

$$t_{\varepsilon 2} = d + \frac{1}{2}\left(d - t_{p2}\right) \tag{8}$$

For J=3, it holds:

$$t_{\varepsilon 3} = 2 \cdot d \cdot \frac{1}{2}\left(d - t_{p3}\right) \tag{9}$$

Generalizing from (7), (8) and (9), for J^{th} interval, we have:

$$t_{\varepsilon J} = \left(J - 1\right) d + \frac{1}{2}\left(d - t_{pJ}\right) \tag{10}$$

Using (6) & (10), we can calculate the duration t_{pJ} and the firing times $t_{\varepsilon J}$. The calculated pulses correspond (in each one of the d intervals) to the average of the related sinusoidal waveform. Ramp time varies from 0 to 10ms for every half period of network waveform.

The flow chart of the proposed PWM strategy is presented in Fig.2.

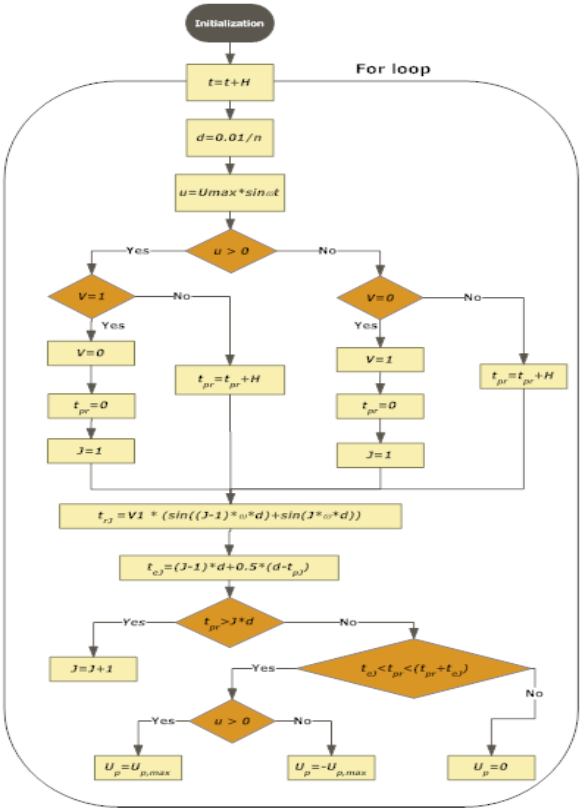

Figure 2**.** Flowchart for the calculation of pulses' duration and firing times for the proposed PWM strategy.

3. SIMULATION

Basic properties of the NPWM are derived by simulation in Matlab (www.mathworks.com) environment. Results for n=3, n=7 and n=15 are presented in Fig.3, Fig.4 and Fig.5 respectively. Pulse durations and firing times for the above values of n are presented in Table I.

TABLE I : Firing times and Pulse Durations for Different Number of Intervals in a Half Period

	$n = 3$		$n = 7$		$n = 15$	
J	t_{eJ}(secs)	t_{rJ}(secs)	t_{eJ}(secs)	t_{rJ}(secs)	t_{eJ}(secs)	t_{rJ}(secs)
1	0.0010251	0.0012831	0.00057654	0.0002755	0.00030253	0.00006161
2	0.0037169	0.0025661	0.0017569	0.00077192	0.00090894	0.00018213
3	0.0076918	0.0012831	0.0030137	0.0011155	0.0015193	0.00029469
4			0.004381	0.0012381	0.0021361	0.00039437
5			0.0058708	0.0011155	0.0027616	0.00047682
6			0.0074712	0.00077192	0.0033975	0.00053842
7			0.009148	0.00027549	0.0040451	0.0005765
8					0.0047053	0.00058938
9					0.0053784	0.0005765
10					0.0060641	0.00053842
11					0.0067616	0.00047681
12					0.0074695	0.00039437
13					0.008186	0.00029469
14					0.0089089	0.00018212
15					0.0096359	0.000061602

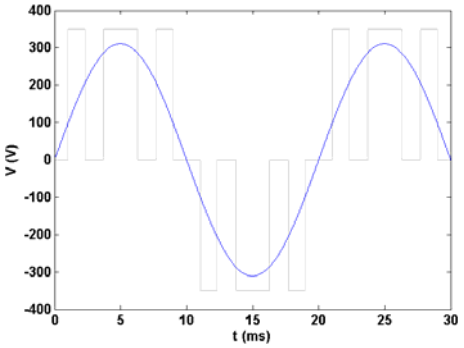

Figure 3.Simulation of network voltage waveform (blue line) by PWM sequence (grey line) for n=3.

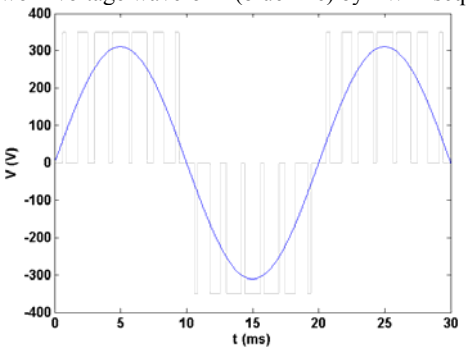

Figure 4. Simulation of network voltage waveform (blue line) by PWM sequence (grey line) for n=7.

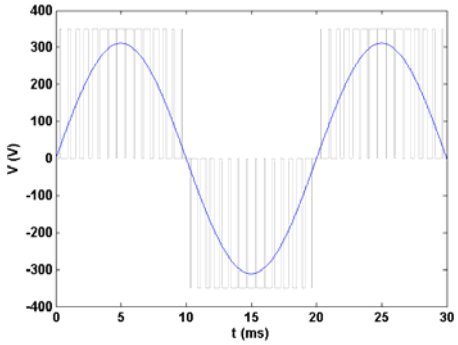

Figure 5. Simulation of network voltage waveform (blue) by PWM sequence (grey line) for n=15.

4. COMPARISON

In order to describe the performance of NPWM we compare it with triangular based PWM in terms of Total Harmonic Distortion (THD).

A typical single phase PWM comparison stage (fundamental frequency f=50Hz, carrier frequency f_c=650Hz, V_{tr}=15V, V_{sin}=12V) produces the waveforms that depicted in Fig.6. The modulation index is $m_{PWM}=12V/15V=0.8$

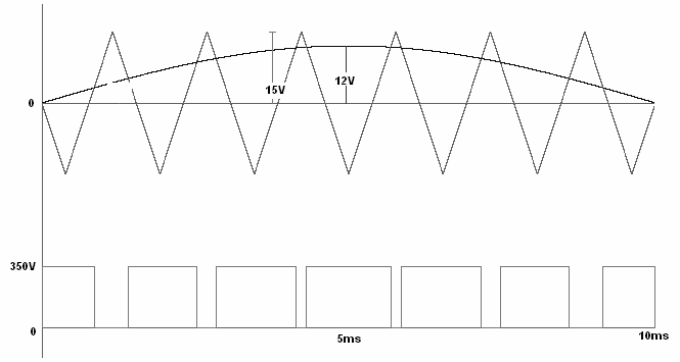

Figure 6. PWM fundamental and carrier waveforms (top) and produced pulse train (bottom) for m_{PWM}=0.8 .

In case of triangular waveform the m_{PWM} selected to be 0.8 as this is the common value found in literature. THD results for odd number of pulses from *n=3* to *n=19* are presented in Fig.7 as diamonds. This modulation index cannot be selected also to the proposed technique because PWM and NPWM produce different modulations since they rely on different modulation principles (i.e. PWM based on comparison between triangular-sine waveform while NPWM based on altering the $U_{max}/U_{p,max}$ ratio in Eq.(6)). For this reason we select as the most reliable criterion the comparison of THDs from equivalent modulation indexes. By term equivalent we refer to the modulation indexes from each technique that produced from pulse trains with equal maximum pulse width (Δt_{max}) around 90^o as depicted in Fig.8. The equivalent m_{NPWM}=0.8889 produces THD results that depicted as triangles in Fig.7.

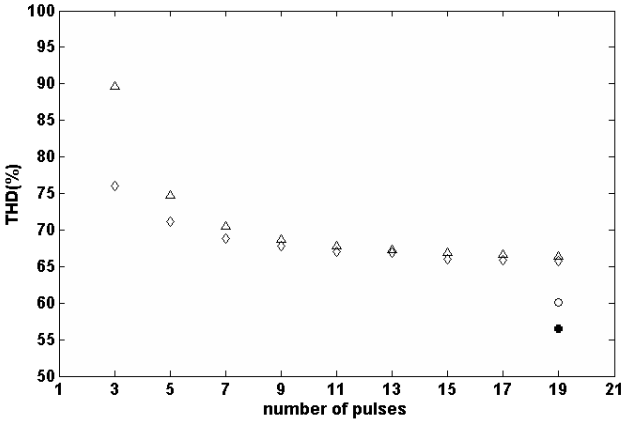

Figure 7. THD vs. number of pulses per period for different modulation indexes. m_{PWM}=0.8 (diamonds), m_{NPWM}=0.8889 (triangles), m_{PWM}=0.89333 (open circle) and m_{NPWM}=0.972 (solid circle).

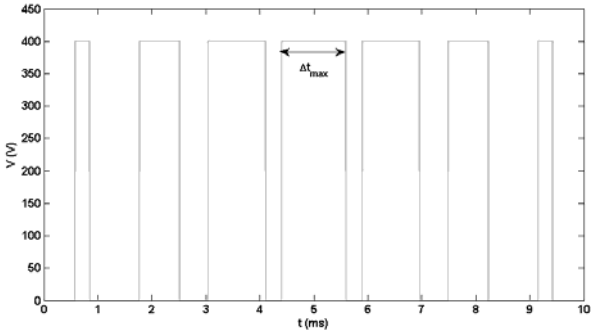

Figure 8. Definition of the maximum pulse width (Δt_{max}) for a pulse train (gray solid line) with odd number (here n=7) of pulses.

The above results indicate that NPWM initially does not perform better than PWM in terms of THD. After experimentation we found that this is not the general case and this situation can be reversed. More specific there is a number of modulation indexes where NPWM presents better or at least equal results than PWM. Such a case is presented in Fig.7 as open circle (for PWM) and solid circle (for NPWM). The results are for *n=19* and equal Δt_{max}=0.51ms around 90^o. The calculated firing times for one period presented in Table II. The estimated modulation indexes are m_{PWM}=0.89333 and m_{NPWM}=0.972. Under these conditions NPWM presents 3.6% lower THD than PWM.

TABLE II : Firing times for n=19 pulses leading to 0.51ms maximum pulse width

t_n	*NPWM (ms)*	**PWM** *(ms)*
1	0.242	0
2	0.284	0.281
3	0.727	0.521
4	0.852	0.842
5	1.213	1.042
6	1.418	1.403
7	1.703	1.565
8	1.982	1.962
9	2.196	2.089
10	2.541	2.518
11	2.694	2.614

12	3.096	3.072
13	3.197	3.143
14	3.645	3.623
15	3.706	3.673
16	4.189	4.171
17	4.222	4.207
18	4.725	4.715
19	4.745	4.745
20	5.255	5.255

5. RESULTS AND DISCUSSION

For the purpose of gathering results for practical applications, a simulation for the circuit depicted in Fig. 9, is performed. This is based in an ordinary topology which used to return power to network from Photovoltaic (P/V) systems and consists of the following main parts: DC Input voltage (U_{in}) from the P/Vs, Bridge (four IGBTs with corresponding diodes), Control Unit (K) and R-L filter.

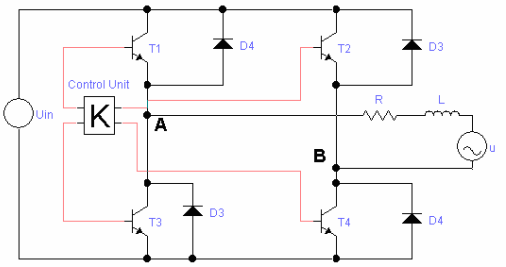

Figure 9. Block diagram of the circuit used to deliver power (from P/V systems) to network. This circuit used for the simulation.

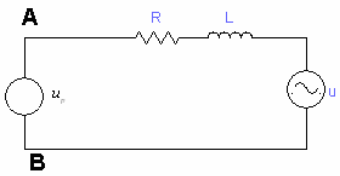

Figure 10. Equivalent circuit of Fig.9.

PWM is generated between points A-B. When $u_{net} > 0$, the IGBTs T1 & T4 operate and when $u_{net} < 0$, the T2 & T3 operate respectively. The equivalent circuit from A-B points can be constructed and is presented in Fig. 10.

From the equivalent circuit the following differential equation can be derived:

$$u_p = Ri + L\frac{di}{dt} + u \Rightarrow L\frac{di}{dt} = -Ri - u + u_p \Rightarrow$$

$$L\frac{di}{dt} = Ri - U_{\max}\sin\omega t + u_p \Rightarrow$$

$$\frac{di}{dt} = -\frac{R}{L}i - \frac{U_{\max}}{L}\sin\omega t + \frac{1}{L}u_p \qquad (11)$$

Where $u = u_{net}$

The solution of differential equation is based on *Runke-Kutta 4* method [17]. u_p is

substituted with PWM sequence. Using R=1Ω (in order to depict current along with voltages), L=0.01H and $U_{net,max}$=311.127V several simulations run varying n from 15 to 90. Results for n=45 are depicted in Fig.11 and for n=15 in Fig.12.

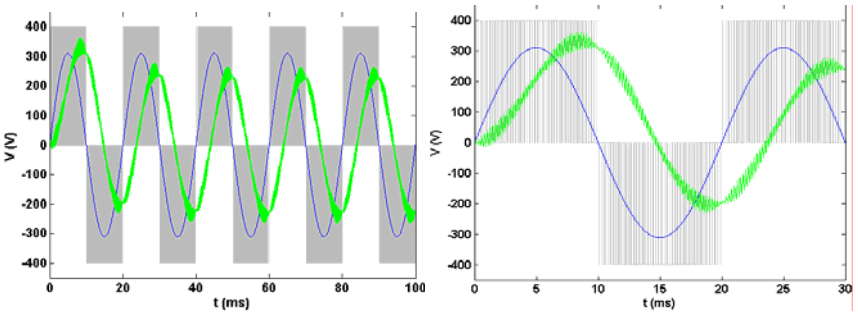

Figure 11. Simulation results for n=45. Network waveform (blue line), produced waveform (green line) and PWM pulse sequence (grey lines). Right plot zooms in interval 0-30ms of left plot.

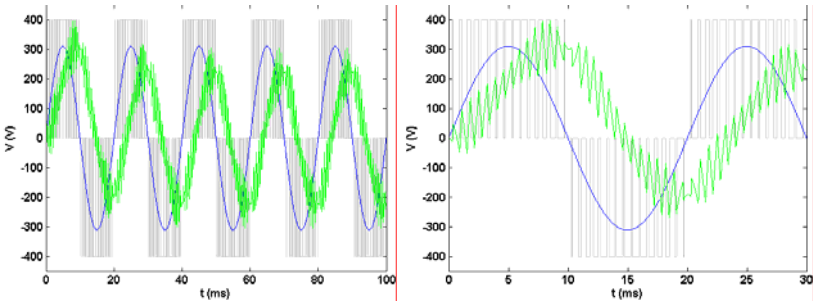

Figure 12. Simulation results for n=15. Right plot zooms in interval 0-30ms of left plot. Grey lines represent PWM pulse sequence.

The initial observation is that the produced waveform presents a significant phase difference with voltage. This leads to a reduced power return to the network. In order to overcome this limitation a phase shift is dictated. At the same time, the remaining parameters must keep their values in order to have the same amplitudes. Our approach is to left shift the PWM sequence in order to produce the required After experimenting, optimum phase angles φ were calculated in order to nullify the phase difference between current and voltage. A typical example of this situation is depicted in Fig.13a where for $n=45$ the optimum φ was found at 22°. We must note that in this case L=0.04mH otherwise the amplitude of the produced waveform will reach higher values.

In case that we decrease n the produced waveform is less smooth than previous situation (where n=45) as depicted in Fig.13b. This could be served as a threshold of the minimum value of n in future studies.

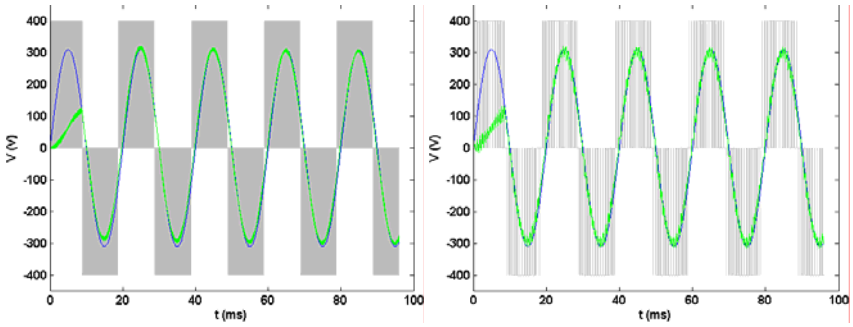

Figure 13. (a) Simulation results for n=45 (left) and (b) for n=15 (right) with φ=22^o and L=0.04H. Voltage (black line) and produced waveform (green line) are in phase. Grey areas represent dense PWM pulse sequence

The practical use of NPWM can be summarized as follows: it can replace the existing control units in conventional PWM based power systems (e.g. in an inverter). It can also be used to interconnect P/V to public power network. The main reasons that NPWM method seems promising against ordinary PWM are the following:

- In terms of THD, NPWM presents better performance or at least equal to ordinary PWM.
- It is a fully mathematical technique in contrary to the triangular-sine comparison in ordinary PWM where the triangular waveform is generated by means of geometric approaches (i.e. by definition of points).
- It is oriented for implementation using modern microprocessor and embedded systems.

5. CONCLUSIONS

A new PWM control strategy for the single phase converter has been proposed and analysed in this paper. The proposed PWM is based on the approximation of sinusoidal waveform by rectilinear segments and their substitution by pulses from a PWM sequence. Theoretical and simulated results were presented verifying the validity of the proposed method. Except the validation of the proposed method, the simulations reveal the problem of phase difference between output voltage and current. This is solved by delaying the PWM sequence in an amount of time defined by the characteristics of the output filter that is going to be used. In our case, with a R=1Ω and L=40mH, a phase angle correction around 22^o was enough.

From a conventional point of view we can earn three main advantages: First, the proposed PWM control strategy is based in a clear and well defined mathematical formulation providing the ability or rapid deployment and transparent configuration. Second, this PWM strategy leads to reduction of components (comparator stages) since it is useful for implementation in modern microprocessors. Third, there is an increase of simplification since there is no need for highly sophisticated algorithms or control circuits.

Future research will focus on two directions: at the implementation of proposed PWM in suitable microprocessor as well as in analysing the performance of the method in several power circuits in comparison with triangle-based PWM.

LIST OF SYMBOLS

- U_{max} : maximum network voltage (here 311.127V)
- ω : angular frequency (here 314.16Hz)
- $u = U_{max} \sin\omega t$:voltage of the signal that is going to be approximated (V)

- U_{dis} : distortion voltage (V)
- n : number of pulses (intervals in a half period)
- d: number of equal intervals used for approximation
- U_j : average voltage in J interval (V)
- t_{pj} : pulse "ON" duration in J interval (*secs*)
- $t_{\bar{e}j}$: pulse "OFF" duration in J interval (*secs*)
- t_{ej} : firing time at J interval (*secs*)
- H : calculation step (here 0.0000001)
- φ : phase angle (degrees)

REFERENCES

[1] Mohan, N, Undelend, T., Robbins, W, "Power electronics converters – Application and design", J.Wiley and sons, USA, 1995.

[2] A. M. Trzynadlowski, "An overview of modern PWM techniques for three-phase, voltage-controlled, voltage-source inverters," in *Proc. IEEE Symp. Industrial Electronics ISIE'96*, pp. 25–39, 1996

[3] J. Holtz, "Pulsewidth modulation—A survey," *IEEE Trans. Ind. Electron.*, vol. 39, pp. 410–420, Oct. 1992.

[4] R.W. Erickson, Fundamental of Power Electronics, Kluwer Academic Publishers, Norwell, MA, 1999.

[5] M.H. Rashid, Power Electronics: Circuits, Devices, and Applications", Pearson Prentice Hall, New Jersey, USA, 2004.

[6] J.-J. Chen, H.-Y. Lin, Y.-T. Lin, W.-Y. Chung, Integrated pulse-width modulation circuit using CMOS processes, in: IEEE 35th Annual Power Electronics Specialists Conference, vol. 2, 20–25, Aachen, Germany, pp. 1356–1358, June 2004

[7] Y.-T. Lin, W.-Y. Chung, D.-S. Wu, K.-S. Chang, J.-J. Chen, Integrated low-voltage pulse-width modulation circuit using CMOS processes, in: The Third International IEEE-NEWCAS Conference, Quebec Canada, pp.163–165, 2005

[8] Z. Lai and K.M. Smedley, A general constant-frequency pulse-width modulator and its applications, *IEEE Trans. Circuits Syst. I: Fund. Theory Appl.* 45 (4) pp. 386–396, 1998.

[9] S.-C. Tan, Y.M. Lai, M.K.H. Cheung, C.K. Tse, A pulse-width modulation based sliding-mode controller for buck converters, in: IEEE 35th Annual Power Electronics Specialists Conference, vol. 5, Aachen, Germany, pp. 3647–3653, June 2004

[10] P. Enjeti and J. F. Lindsay, "Solving nonlinear equation of harmonic elimination PWM in power control," *Electron. Lett.*, vol. 23, no. 12, pp. 656–657, 1987.

[11] S. R. Bowes and R. I. Bullough, "Novel PWM controlled series-connected current-source inverter drive," *Proc. Inst. Elect. Eng. B*, vol. 136, no. 2, pp. 69–82, 1989.

[12] C.-H. Tso, J.-C. Wu, An integrated digital PWM DC/DC converter using proportional current feedback, in: Proceedings of the IEEE International Symposium on Circuits and Systems, vol. 3, Sydney, Australia, pp. III65–III68, 6–9 May 2001,

[13] A.M. Wu, J. Xiao, D. Markovic, S.R. Sanders, Digital PWM control: application in voltage regulation modules, in: Proceedings of the IEEE 30th Annual Power Electronics Specialists Conference, vol. 1, Charleston, pp. 77–83, 1999

[14] C.F. Lee and P.K.T. Mok, A monolithic current-mode CMOS DC–DC converter with on-chip current-sensing technique, *IEEE J. Solid-State Circuits* 39 (1) pp. 3–14, 2004.

[15] C.Y. Leung, P.K.T. Leung, K. Nang and M. Chan, An integrated CMOS current-sensing circuit for low-voltage current-mode buck regulator, *IEEE Trans. Circuits Syst.–II: Express Brief* 52 (7), pp. 394–397, 2005.

[16] J.-J. Chen, Y.-T. Lin, H.-Y. Lin, J.-H. Su, W.-Y. Chung, Y.-S. Hwang and C.-L. Tseng, On-chip current sensing technique for hysteresis current controlled DC–DC converters, *IEE Electron. Lett.* 41 (2). pp. 95–97, 2005.

[17] Ernst Hairer, Syvert Paul Nørsett, and Gerhard Wanner. *Solving ordinary differential equations I: Nonstiff problems*, second edition. Berlin: Springer Verlag, 1993.